International Journal of Advancements in Electronics and Electrical Engineering – IJCNS
Copyright © Institute of Research Engineers and Doctors
Volume 8 : Issue 2 - [ISSN : 2250-3757] - Publication Date: 27 Dec, 2019

Optimization of Energy Saving Control for Air Conditioning System in Data Center

Leehter Yao and Jin-Hao Huang

***Abstract*—A multi-objective optimization scheme is proposed for energy saving control of both chillers and air handling units (AHUs). The control scheme also maintains rack intake temperature within a specified range. The non-dominated sorting genetic algorithm II (NSGA-II) is utilized to solve the multi-objective optimization problem. In order for every chromosome of NSGA-II to calculate the fitness functions which are both total power of chillers and deviations of AHU outlet cold air temperature from specified range, neural network models are used to model the power consumptions of chillers and AHUs as well as the AHU outlet cold air temperature.**

***Index Terms*—data center, chiller, air handling unit, multi-objective optimization, power usage effectiveness (PUE), rack cooling index (RCI).**

I. Introduction

Following the increasing demand of IOT, big data, cloud computing, artificial intelligence, etc., more and more servers are put into data center. The computing capability of server has also greatly improved over past several years. A great deal of heat exhaust is made as servers and communication facilities operate. However, constant low temperature and humidity are required to be maintained in the data center so that the facilities in data can operate in a normal condition [1-2]. Delicate air conditioning system is usually installed in the data center taking away heat exhaust. The air conditioning system is designed not only to maintain constant indoor temperature and humidity, the heat exhaust from every rack of server cabinet also needs to be removed right away. The delicate air conditioning system installed in data center usually consumes a lot of power. The power consumption of air conditioning system for data center usually could occupy as high as 40% of the total power. Over the past decade, more and more guidelines or even standards building an energy efficient data center have been introduced [3]. Different levels of power usage effectiveness (PUE) indices for data center have also been proposed [4-6]. Improving power usage effectiveness has become a big challenge for scientists and engineers in this area. Air conditioning system is therefore the main target in order to improve the PUE of data center.

Computational field dynamics (CFD) technique has been utilized to simulate airflow distribution and thermal distribution in the data center [7]. In [8-10], different efficient air management and air conditioning system control approaches have been proposed to improve the power usage in data centers. Airflow distribution techniques for data center have been investigated in [11-12] in order to optimize energy usage. Different air management schemes through cold aisle with fan-assisted perforations have been proposed to improve AHU energy efficiency [13-15]. Apart from air management approaches, there have been some intelligent control as well as multi-variable control schemes applied to heat ventilation air conditioning (HVAC) systems, which can be applied to the air conditioning system in data center. Multivariable controller have been designed to control AHU in [16-17] and chiller in [18] in order to save energy for air conditioning system.

A multi-objective optimization approach will be proposed in this paper minimizing power consumption of air conditioning system while keep every rack intake temperature within a specified range. The power consumption of air conditioning system mainly comes from the chiller and AHU. Therefore, both facilities are the main targets for energy saving control. The proposed multi-objective optimization approach will calculate the optimal setting values of the chilled water outlet temperature for chiller as well as the optimal setting values of running speed for AHU fans at every sampling interval. If energy saving control is applied saving too much energy, the rack intake temperature may rise and affect heat exhaust removal for servers. The optimization is thus designed aiming to maintain the rack intake temperature within specified range in addition to saving energy for both chillers and AHUs. However, it is impractical to monitor and control intake temperature of every rack. Since AHU outlet cold air temperature directly influences intake temperature of every rack, it is monitored and utilized as the second objective for optimization.

Since multi-objective optimization for HVAC system is usually a non-convex and nonlinear problem [19], random optimization approach such as genetic algorithm (GA) [20], particle-swarm optimization (PSO) [21], evolutionary algorithm (EA) [22] are commonly utilized. The non-dominated sorting genetic algorithm II (NSGA-II) [23] is applied in this paper for multi-objective optimization. As the convergent pareto-optimal solutions are obtained by NSGA-II, the PUE [4-6] and rack cooling index (RCI) [24-25] are integrated as the criteria selecting the final optimal solutions so that both the energy saving effectiveness is guaranteed with PUE in a specified range, and rack intake temperature is maintained within a specified range. It will be shown in the

The authors are with the Department of Electrical Engineering, National Taipei University of Technology, Taipei 10648, Taiwan..

experiment that the proposed optimization approach not only saves energy for air conditioning system, the rack intake temperature is also kept within a specified range satisfying internationally standardized RCI.

II. Problem Statement and Air Conditioning System of Data Center

The most energy consuming facilities in the data center air conditioning system are mainly air handling units and chillers. The energy saving control for the air conditioning system thus aims to these two main facilities. It is shown in Fig. 1 that hot and cold air aisle configuration is used in the data center. The cold air is driven by the air handling unit (AHU) through the air duct under floor. The hot air exhausted from the server cabinet is circulated through hot air ducts above the ceiling of data center back to AHU. The hot air returned to AHU is cooled down through the chilled water pumped from the chiller to AHU. The server cabinets in data center are lined up in alternating rows with cold air intakes facing one side and hot air exhausts facing the other. The cold/hot air circulation in the data center depends on the speed of fans in the AHU while the cooling temperature of returned hot air depends on the temperature of chilled water. Therefore, the energy saving control for the air conditioning system in data center relies on the control of fan speed of AHU and the temperature of output chilled water from the chiller.

It is straightforward to reduce power consumption of AHU and chiller in order to save energy for data center. However, data center is an environment sensitive to temperature changes. It is easy to increase indoor temperature with inappropriate energy saving control schemes applied to AHU and chiller. A real-time multi-objective optimization approach is to be implemented in energy saving controller (ESC) as in Fig. 1 simultaneously reducing energy and stabilizing intake temperature at every rack. The intake temperature at every rack is directly influenced by AHU cold air outlet temperature.

A commonly used metric called power usage effectiveness (PUE) [4-6] measuring energy efficiency of data center is adopted in this paper showing energy saving effectiveness. PUE is defined as the ratio of total energy consumed by all facilities in data center to the energy consumed by servers and other computing facilities. Denote P_i as the power consumption of the *i-th* facility in data center, P_{AC} as the power consumption of air conditioning system and P_{IT} as the power consumption due to servers and other computing facilities, then

$$\text{PUE}=\frac{\sum_i P_i}{P_{IT}}=\frac{P_{AC}+\sum_{i,i\neq AC} P_i}{P_{IT}}. \tag{1}$$

The energy saving scheme mainly focus on reducing power consumption of chiller and AHU leading to reducing the PUE according to (1). Therefore, PUE is a suitable index to measure the effectiveness of energy saving in this paper.

In order to evaluate influence of energy saving on every rack intake temperature, a metric called rack cooling index (RCI) [24-25] is used in this paper. Let *N* be the total number of intakes in all servers, $T_{\max-all}$ and $T_{\min-all}$ be the maximum and minimum allowable temperature, $T_{\max-rec}$ and $T_{\min-rec}$ be the maximum and minimum recommended temperature, and T_i be the average temperature at the *i-th* intake. According to [24], RCI_{HI} and RCI_{LO} are respectively defined as:

$$RCI_{HI}=(1-\frac{\sum_i (T_i-T_{\max-rec})\big|_{T_i>T_{\max-rec}}}{N(T_{\max-all}-T_{\max-rec})})\ 100\%\ ; \tag{2}$$

$$RCI_{LO}=(1-\frac{\sum_i (T_{\min-rec}-T_i)\big|_{T_i<T_{\min-rec}}}{N(T_{\min-rec}-T_{\min-all})})\ 100\%\ . \tag{3}$$

RCI_{HI} and RCI_{LO} are indices measuring intakes being over-temperature and under-temperature, respectively. It is reasonable to expect that most of RCI_{LO} are 100% because energy saving of air conditioning system may lead to intake temperature increasing instead of decreasing.

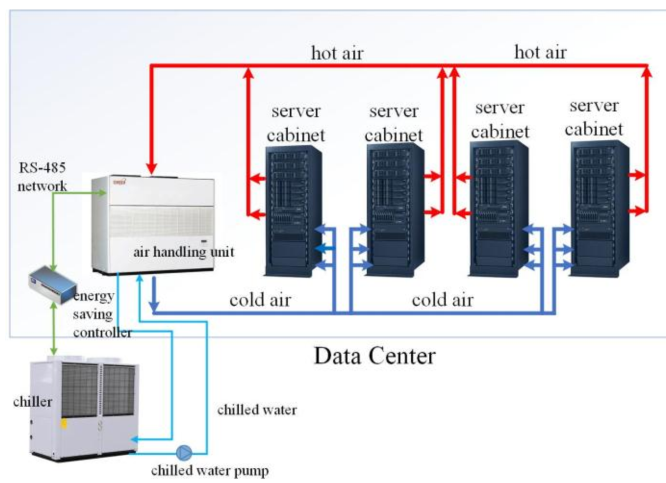

Fig. 1. System structure of energy saving control of air conditioning system in data center

III. Multi-objective Optimization

The most energy-consuming facilities in the data center air conditioning system are chiller and AHU. Denote $P_{ch}(k)$ and $P_{AHU}(k)$ as the power of chiller and AHU, respectively, at the *k-th* time step. The proposed energy saving scheme aims to minimize the total power as following:

$$P_{AC}(k)=P_{ch}(k)+P_{AHU}(k). \tag{4}$$

In parallel with minimizing $P_{AC}(k)$, every rack intake temperature needs to maintained within a preset range. Referring to Fig. 1, all rack intake temperatures depend on AHU outlet cold air temperature $T_f(k)$. Assume that $T_f(k)$ is

International Journal of Advancements in Electronics and Electrical Engineering – IJCNS
Copyright © Institute of Research Engineers and Doctors
Volume 8 : Issue 2 - [ISSN : 2250-3757] - Publication Date: 27 Dec, 2019

maintained within the range between T_f^L and T_f^U, i.e., $T_f^L \le T_f(k) \le T_f^U$. Define the temperature difference $T_d(\cdot)$ as:

$$T_d(k) = \max\left(0, \left(T_f^L - T_f(k)\right)\right) + \max\left(0, \left(T_f(k) - T_f^U\right)\right). \quad (5)$$

By controlling the chilled water outlet temperature $T_{chwo}(k)$ of chiller as well as running speed of AHU fans $v_f(k)$, two objectives are to be optimized, i.e., the power consumption $P_{AC}(k)$ as well as the temperature difference $T_d(k)$ at every *k-th* time step. The energy saving control scheme is to search for the optimal settings $T_{chwo}^*(k)$ and $v_f^*(k)$ at every *k-th* time step. Therefore,

$$\left(T_{chwo}^*(k), v_f^*(k)\right) = \underset{T_{chwo}(k), v_f(k)}{\arg\min} \left(P_{AC}(k), T_d(k)\right). \quad (6)$$

subject to:

$$T_{chwo}^L \le T_{chwo}(k) \le T_{chwo}^H; \quad (7)$$

$$v_f^L \le v_f(k) \le v_f^U. \quad (8)$$

Note that T_{chwo}^L and T_{chwo}^H are lower and higher limit respectively, for $T_{chwo}(k)$ in accordance with chiller's operation characteristics. Similarly, v_f^L and v_f^H are lower and higher limit respectively, for $v_f(k)$ in accordance with AHU's operation characteristics. The multi-objective optimization in (6) with the constraints in (7)-(8) is calculated by ESC using NSGA-II at every time step. Most of chillers are with interfaces allowing remote setting of chilled water outlet temperature $T_{chwo}(k)$. Similarly, most of AHUs are also with interfaces allowing remote setting of running speed of AHU fans $v_f(k)$. Referring to Fig. 1, ESC is designed to conduct the remote setting with most commonly used RS-485 network. Other wired or wireless network such as Ethernet, Wifi, Zigbee, etc. can also be used to replace RS-485 network.

IV. NSGA-II and Neural Network Models

NSGA-II is utilized to implement the multi-objective optimization in (6)-(8). Both the optimization variables $T_{chwo}(k)$ and $v_f(k)$ are parameterized in the chromosome in real numbers. Both objective functions in (6), i.e., $P_{AC}(k)$ and $T_d(k)$, are utilized as the fitness functions. Referring to (4), $P_{AC}(k)$ is calculated based on the power consumption of chiller and AHU, i.e., $P_{ch}(k)$ and $P_{AHU}(k)$. For on-line learning of NSGA-II, it is not possible to practically measure both $P_{ch}(k)$ and $P_{AHU}(k)$ corresponding to different optimization variables $T_{chwo}(k)$ and $v_f(k)$ encoded by the chromosomes in gene pool. A feedforward neural networks (FNN) based model is learned a priori based on the recorded data so that $P_{ch}(k)$ and $P_{AHU}(k)$ can be estimated corresponding to different set of optimization variables encoded in the chromosome as well as some variables measured on-line.

Denote ρ_f as the flow rate of chilled water, c_w as the specific heat capacity of water, the chilled water inlet temperature of chiller as $T_{chwi}(k)$. The cooling capacity *Q* of a chiller is calculated as following:

$$Q(k) = \rho_f c_w \left(T_{chwi}(k) - T_{chwo}(k)\right). \quad (9)$$

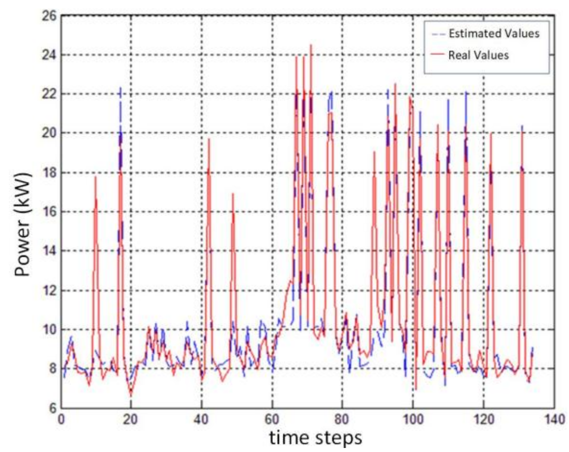

(a)

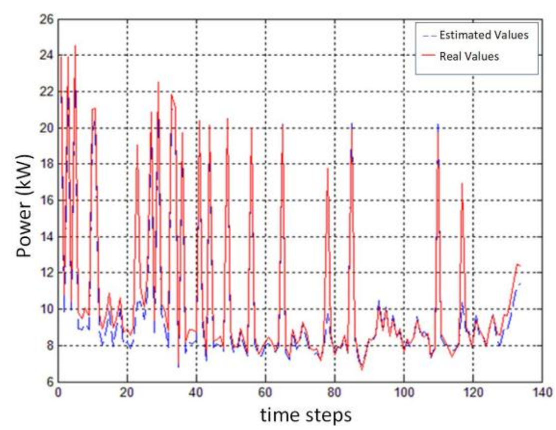

(b)

Fig. 2. Comparison of chiller power consumptions between estimated and real values for (a)chiller 1, (b) chiller 2.

Therefore, $P_{ch}(k)$ directly depends on the value of $\left(T_{chwi}(k) - T_{chwo}(k)\right)$ according to (9). By recording 12 months of chiller power consumption $P_{ch}(k)$ and chiller's different combinations of chilled water inlet and outlet temperatures $T_{chwi}(k)$ and $T_{chwo}(k)$, $P_{ch}(k)$ can be expressed as a function of $\left(T_{chwi}(k) - T_{chwo}(k)\right)$. Denote this function as Γ_{ch} which is learned and modeled by an FNN. $P_{ch}(k)$ can be expressed in association with Γ_{ch} as:

$$P_{ch}(k) = \Gamma_{ch}\left(T_{chwi}(k) - T_{chwo}(k)\right). \tag{10}$$

The function Γ_{ch} is implemented as a 1×10×10×1 FNN with 1 input, 1 output and 2 hidden layers with 10 neurons per layer. Back propagation is utilized as the learning approach. In order to test the modeling capability, a typical unlearned day is selected for testing. It is shown in Fig. 2 that the comparison between the estimated chiller power consumption and the real data are very closed for both #1 and #2 chillers. For on-learning, the chilled water inlet temperature $T_{chwi}(k)$ is directly measured by sensors while $T_{chwo}(k)$ is the optimization variable encoded in the chromosome.

The running speed of AHU fans $v_f(k)$ is usually adjusted through PWM controller. Similar to the model for chiller, the relationship between $P_{AHU}(k)$ and $v_f(k)$ can also be learned and modeled by an FNN. Denote Γ_f as the function modeling this relationship, then $P_{AHU}(k)$ can be expressed as:

$$P_f(k) = \Gamma_f\left(v_f(k)\right). \tag{11}$$

The function Γ_f is implemented as a 1×10×1 FNN with 1 input, 1 output and 1 hidden layers with 10 neurons. Γ_f is learned with the recorded 12 months of training data between $P_{AHU}(k)$ and $v_f(k)$ using back propagation. A typical unlearned day is selected in order to test the modeling capability. Fig. 3 shows that the estimated and real data for AHU power consumption are closed.

As for the calculation of second objective $T_d(k)$ in (5), a model estimating AHU outlet cold air temperature $T_f(k)$ is essential. Different from the models for $P_{ch}(k)$ and $P_f(k)$, any changes in the inputs of these two models are directly reflected to the outputs without time delay. It takes time for $T_f(k)$ to change. Moreover, any changes in the AHU outlet cold air temperature are also related to the temperatures in previous time steps. It is assumed in this paper that $T_f(k+1)$ are related to the temperatures in previous two time steps, i.e., $T_f(k)$ and $T_f(k-1)$. Although data center is a closed environment, $T_f(k)$ is still affected by the outdoor temperature because the air-cooling chillers are installed outdoor. Therefore, $T_f(k)$ also depends on the outdoor temperature $T_o(k)$ which can be measured by a temperature sensor. Finally, both optimization variables $T_{chwo}(k)$ and $v_f(k)$ determined at every *k-th* time step also affect $T_f(k)$. Similar to previous modeling approaches, denote Γ_{tmp} as a function modeling the relationship between $T_f(k+1)$ and other elements including $T_f(k)$, $T_f(k-1)$, $T_o(k)$, $T_{chwo}(k)$ and $v_f(k)$. Therefore,

$$T_f(k+1) = \Gamma_{tmp}\left(T_f(k), T_f(k-1), T_o(k), T_{chwo}(k), v_f(k)\right). \tag{12}$$

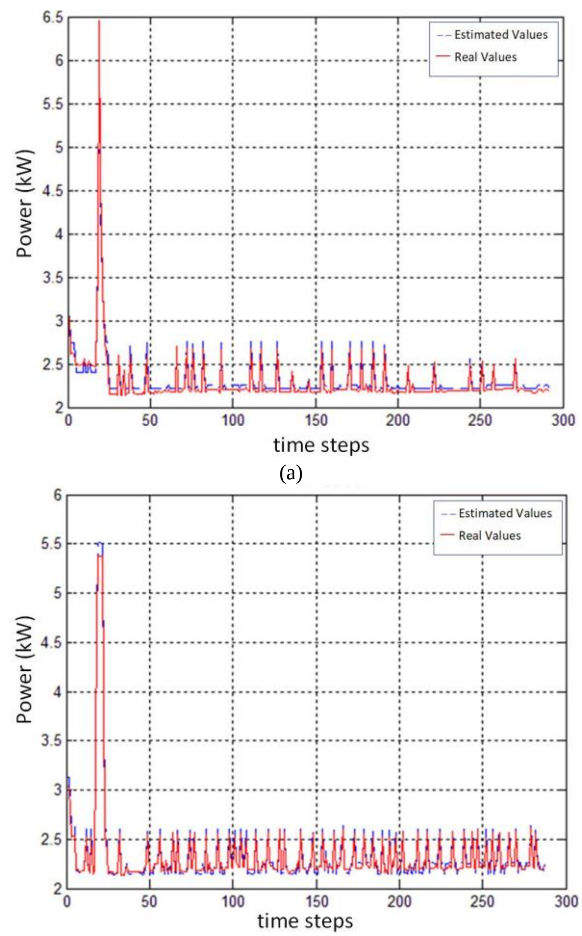

(a)

(b)

Fig. 3. Comparison of AHU power consumptions between estimated and real values for (a)AHU 1, (b) AHU 2.

A 1×15×15×1 FNN with 5 inputs, 1 output and 2 hidden layers with 15 neurons per layer is utilized to model Γ_{tmp}. Γ_{tmp} is also learned based on recorded 12 months of training data between inputs and output. A typical unlearned day is selected and tested the modeling performance. Fig. 4 shows good performance of temperature prediction by Γ_{tmp}.

After the convergent pareto-optimal solutions of the multi-objective optimization problem in (6-8) are achieved, the solution to the problem is obtained by searching all pareto-optimal solutions based on PUE and RCI. Denote $\boldsymbol{x}$ as the pareto-optimal solution and $P(\boldsymbol{x})$ as the set all pareto-optimal solutions, $\boldsymbol{x} \in P(\boldsymbol{x})$. Let $B_1(\boldsymbol{x}) \subset P(\boldsymbol{x})$ be the subset of pareto-optimal solutions leading to PUE satisfying a specified range, i.e.

$$B_1(\boldsymbol{x}) = \left\{ \boldsymbol{x} \middle| \boldsymbol{x} \in P(\boldsymbol{x}), \rho^L \le PUE \le \rho^H \right\}, \tag{13}$$

where ρ^L and ρ^H are lower and upper bound assigned to PUE. Similarly, let $B_2(\boldsymbol{x}) \subset P(\boldsymbol{x})$ be the subset of pareto-optimal solutions leading to both RCI indices satisfying specified ranges, i.e.

$$B_2(\boldsymbol{x}) = \left\{ \boldsymbol{x} \middle| \boldsymbol{x} \in P(\boldsymbol{x}), \sigma_{LO}^L \le RCI_{LO} \le \sigma_{LO}^H, \sigma_{HI}^L \le RCI_{HI} \le \sigma_{HI}^H \right\} \tag{14}$$

where σ_{LO}^L and σ_{LO}^H are the lower and upper bound assigned to the index RCI_{LO} while σ_{HI}^L and σ_{HI}^H are the lower and upper bound assigned to the index RCI_{HI}. The solutions $\boldsymbol{x} \in P(\boldsymbol{x})$ to the proposed problem thus satisfies the condition:

$$\boldsymbol{x} \in \left(B_1(\boldsymbol{x}) \cap B_2(\boldsymbol{x}) \right). \tag{15}$$

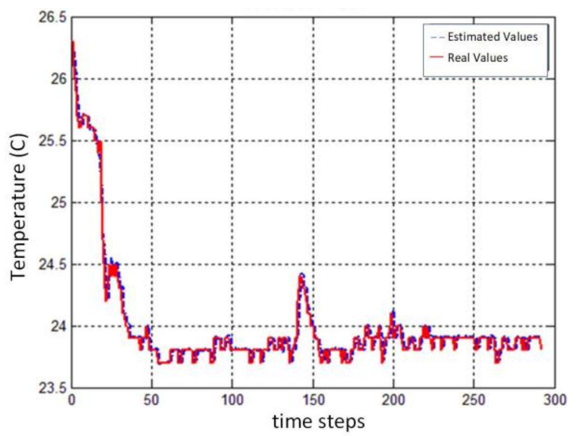

(a)

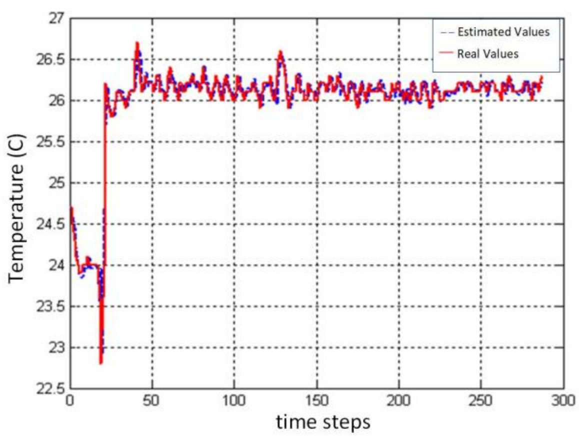

(b)

Fig. 3. Comparison of predicted and real AHU outlet cold air temperature for (a)AHU 1, (b) AHU 2.

V. Experiments

The air conditioning system for the experiment consists of two AHUs and two chillers. One chiller and one AHU are controlled by the proposed multivariable objective energy saving control scheme while the other AHU and chiller are left uncontrolled providing baseload. The lower and upper bounds for some variables are set as following: $T_f^L = 23.5$, $T_f^H = 24.5$; $T_{chwo}^L = 7$, $T_{chwo}^H = 12$; $v_f^L = 50\%$, $v_f^H = 100\%$; $\rho^L = 1.4$, $\rho^H = 1.7$; $\sigma_{LO}^L = 0.96$, $\sigma_{LO}^H = 1.0$; $\sigma_{HI}^L = 0.92$, $\sigma_{HI}^H = 1.0$. The constants for RCI in (2) and (3) are set as following according to [3]: $T_{\max-rec} = 27$, $T_{\max-all} = 32$, $T_{\min-rec} = 18$, $T_{\min-all} = 15$. As for NSGA-II, the parameters are set as following: the maximum allowed iterations = 80, the number of chromosomes in the gene pool = 50, crossover rate = 0.8, mutation rate = 0.05, crossover distribution index = 20, mutation distribution index = 20.

In order to verify the effectiveness and proposed control scheme, the control scheme was applied from 19:50 to 23:50 on one summer night. The control interval is set as 15 minutes. In other words, the proposed multi-objective optimization approach is executed and the optimization variables: chilled water outlet temperature T_{chwo} of chiller as well as running speed of AHU fans v_f are both calculated and updated every 15 minutes. It takes about 120 seconds for the ESC running the proposed multi-objective optimization and returns the updated values for both optimization variables T_{chwo} and v_f.

The variation of outdoor temperature is shown in Fig. 4. For the convenience of illustration, vertical black bars are added in Fig. 5-7 showing the start and end of control interval. It is shown in Fig. 5 that the AHU outlet cold air temperature T_f starts dropping as soon as the control scheme is applied at 19:50 and goes up as soon as the control interval ends. The reason T_f goes down during the control interval is because the control scheme also requires that RCI indices in (2)-(3) satisfy the specified ranges in (14). Fig. 6 shows that the variations of T_{chwo} calculated by the proposed multi-objective optimization approach and the measured chilled water outlet temperature. The measured values did follow the calculated ones.

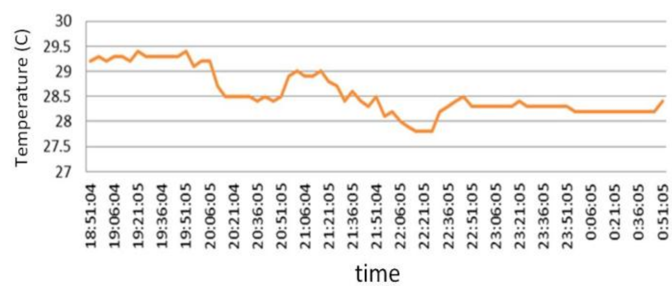

Fig. 4. Outdoor temperature.

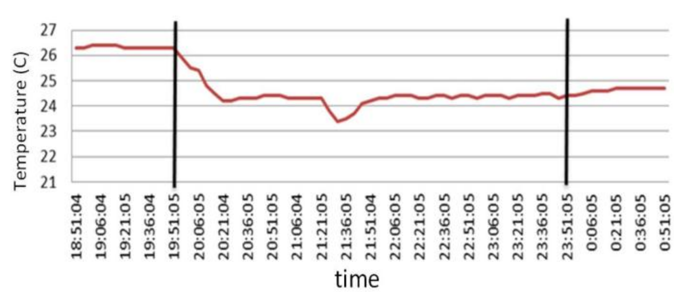

Fig. 5. AHU outlet cold air temperature.

In response to the calculated and measured chilled water outlet temperature, the chiller power consumption did go down as the control interval starts and return as the control interval ends showing the effectiveness of energy reduction performance of the proposed control scheme. Since the running speed v_f of AHU fans is adjusted by PWM controller, the variation of calculated v_f is shown in duty cycles as shown in Fig. 7. Referring to Fig. 7, the power consumption within the control interval slightly increases. It leads to AHU outlet cold air temperature T_f goes down within the control interval as shown in Fig. 5. Although AHU power consumption slightly increased, chiller power consumption goes down during the control interval. In total power consumption of both chiller and AHU is shown in Fig. 8. It is shown in Fig. 8 that the total power did goes down within the control interval. The PUE before the control interval is 1.55 and yet the PUE within the control interval drops to 1.42. The RCI_{LO} and RCI_{HI} before the control interval is applied are 100% and 93%, respectively, while both values are 100% within the control interval.

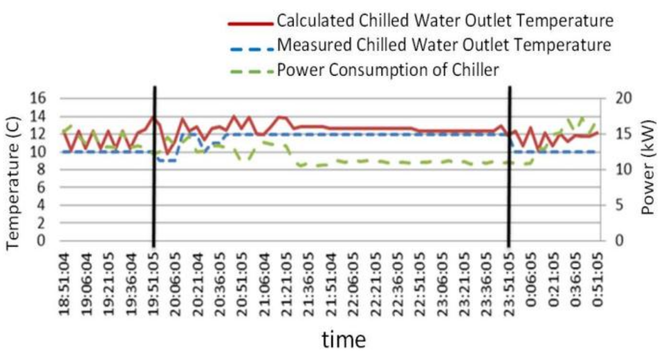

Fig. 6. Calculated and measured chilled water outlet temperature and chiller power consumption.

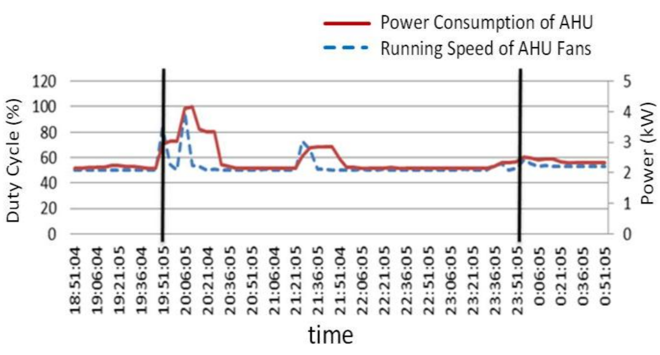

Fig. 7. Running speed of AHU fans and AHU power consumption.

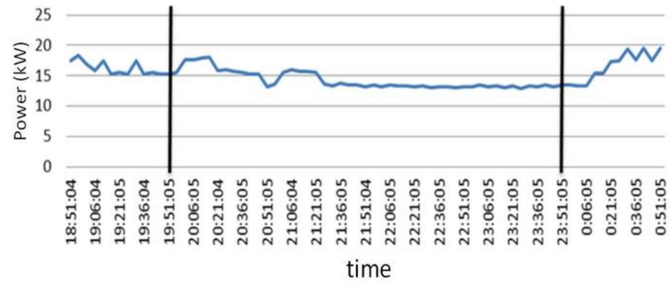

Fig. 8. Total power consumption of chiller and AHU.

VI. Conclusion

A multi-objective optimization approach has been proposed to optimize the energy saving effectiveness. The optimization approach minimize the power consumptions of both chillers and AHUs while keeping AHU outlet cold air temperature within a specified range. Both commonly used standardized indices for data center including PUE and RCI are utilized as the criteria to further select final optimal solutions from among pareto-optimal solutions obtained by NSGA-II. In fact, the proposed control scheme can also be applied to other central air conditioning system controlling both chillers and AHUs. FNN is utilized for the prediction of AHU outlet cold air temperature. Other models such as recurrent neural network (RNN) and long short-term memory (LSTM) can also be used if the size of data center is too large and/or the air distance is too long for FNN.

References

[1] E. M. Shehabi, H. Price, A. Horvath, and W. W. Nazaroff, “Data center design and location: consequences for electricity use and greenhouse-gas emission,” *Building and Environment*, vol. 46, pp. 990-998, 2011.

[2] J. Cho and B. S. Kim, “Evaluation of air management systems’ thermal performance for superior cooling efficiency in high density data centers,” Energy and Buildings, vol. 43, pp. 2145-2155, 2011.

[3] ASHRAE, *ASHRAE Guidelines for Data Processing Environments*, 2011.

[4] V. Avelar, D. Azevedo, and A. French, “PUE: A comprehensive examination of the metric,” White Paper #49, The Green Grid, 2012.

[5] J. Yuventi and R. Mehdizadeh, “A critical analysis of power usage effectiveness and its use in communicating data center energy consumption,” *Energy and Buildings*, vol. 64, pp. 90-94, 2013.

[6] G. Brady, N. Kapur, J. Summers, and H. Thompson, “A case study and critical assessment in calculating power usage effectiveness for a data center,” *Energy Conversion & Management*, vol. 76, pp. 155-161, 2013.

[7] C. E. Bash, C. D. Patel, and R. K. Sharma, “Efficient thermal management of data centers-immediate and long-term research needs,” *HVAC&R Research*, vol. 9, pp. 137-152, 2003.

[8] B. Fakhim, M. Behnia, S. W. Armfield, and N. Srinarayana, “Cooling solutions in an operational data centre: a case study,” *Applied Thermal Engineering*, vol. 31, pp. 2279-2291, 2011.

[9] J. F. Karlsson and B. Moshfegh, “Investigation of indoor climate and power usage in a data center,” *Energy and Buildings*, vol. 37, pp. 1075-1083, 2005.

[10] T. Lu, X. S. Lu, M. Remes, and M. Vijanen, “Investigation of air management and energy performance in a data center in Finland: case study,” *Energy and Buildings*, vol. 43, pp. 3360-3372, 2011.

[11] J. Cho, T. Lim, and B. S. Kim, “Measurements and predictions of the air distribution systems in high computer density (Internet) data centers,” Energy and Buildings, vol. 41, pp. 1107-1115, 2009.

[12] H. E. Khalifa and D. W. Demetriou, “Energy optimization of air-cooled data centers,” *Thermal Science and Engineering Applications*, vol. 2, pp. 1-13, 2010.

[13] V. K. Arghode, V. Sundaralingam, and Y. Joshi, “Airflow management in a contained cold aisle using active fan tiles for energy efficient

data-center operation," *Heat Transfer Engineering*, vol. 37, pp. 246-256, 2016.

[14] Z. Song, "Numerical cooling performance evaluation of fan-assisted perforations in a raised-floor data center," *International Journal of Heat Mass Transfer*, vol. 95, pp. 833-842, 2016.

[15] Z. Song, "Thermal performance of a contained data center with fan-assisted perforations," *Applied Thermal Engineering*, vol. 102, pp. 1175-1184, 2016.

[16] Qi. Qi, and S. M. Deng, "Multivariable control of indoor air temperature and humidity in a direct expansion (DX) air conditioning (A/C) system, " *Building and Environment*, vol. 44, no. 8, pp. 1659-1667, 2009.

[17] M.W. Khan, M.A. Choudhry, M. Zeeshan, and A. Ali, "Adaptive fuzzy multivariable controller design based on genetic algorithm for an air handling unit," *Energy*, no. 81, pp. 477–488, 2015.

[18] Y. C. Chang, W. H. Chen, C. Y. Lee, and C. N. Huang, "Simulated annealing based optimal chiller loading for saving energy," *Energy Conversion and Management*, vol. 47, pp. 2044–2058, 2006.

[19] X. Wei, A. Kusiak, M. Li, F. Tang, and Y. Zeng, "Multi-objective optimization of the HVAC (heating, ventilation, and air conditioning) system performance," *Energy*, vol. 83, pp. 294-306, 2015.

[20] G. X. Kusiak and F. Tang, "Optimization of an HVAC system with a strength multi-objective particle-swarm algorithm," *Energy*, vol. 36, no. 10, pp. 5935-5943, 2011.

[21] L. Magnier, and F. Haghighat, "Multiobjective optimization of building design using TRNSYS simulations, genetic algorithm, and Artificial Neural Network," *Building and Environment*, vol. 45, no. 3, pp. 739-746, 2010.

[22] F. T. Kusiak, and G. Xu, "Multi-objective optimization of HVAC system with an evolutionary computation algorithm," *Energy*, vol. 36, no. 5, pp.2440-2449, 2011.

[23] K. Deb, A. Pratap, S. Agarwal, and T. Meyarivan. "A fast and elitist multiobjective genetic algorithm: NSGA-II," *IEEE Transaction on Evolutionary Computation*, vol. 6, no.2, pp. 182-197, 2002.

[24] M. K. Herrlin, "Rack cooling effectiveness in data centers and telecom central offices: The rack cooling index (RCI)," *ASHRAE Transactions*, vol. 111, pp. 725-731, 2005.

[25] B. Norouzi-Khangah, M. B. Mohammadsadeghi-Zzad, S. M. Hoseyni, and S. M. Hoseyni, "Performance assessment of cooling systems in data centers; Methodology and application of a new thermal metric," *Case Studies in Thermal Engineering*, vol. 8, pp. 152-163, 2016.